Optimized operation of dielectric laser accelerators: Multibunch

Adi Hanuka* and Levi Schächter

Department of Electrical Engineering, Technion–Israel Institute of Technology, Haifa 32000, Israel

(Received 10 September 2017; published 7 June 2018)

We present a self-consistent analysis to determine the optimal charge, gradient, and efficiency for laser driven accelerators operating with a train of microbunches. Specifically, we account for the beam loading reduction on the material occurring at the dielectric-vacuum interface. In the case of a train of microbunches, such beam loading effect could be detrimental due to energy spread, however this may be compensated by a tapered laser pulse. We ultimately propose an optimization procedure with an analytical solution for group velocity which equals to half the speed of light. This optimization results in a maximum efficiency 20% lower than the single bunch case, and a total accelerated charge of 10^6 electrons in the train. The approach holds promise for improving operations of dielectric laser accelerators and may have an impact on emerging laser accelerators driven by high-power optical lasers.

DOI: 10.1103/PhysRevAccelBeams.21.064402

I. INTRODUCTION

In the past two decades direct electron acceleration driven by laser was experimentally demonstrated. Bounded by gradient limitations (∼100 MV/m), it has been shown [1–3] that net acceleration could be achieved by a train of microbunches spaced at the optical period. However, some applications require significantly higher accelerating gradients than provided by conventional rf linear accelerators, such as compact radiotherapy devices [4] and miniaturized light sources [5,6].

Dielectric laser accelerator (DLA) structures have the potential to facilitate higher gradients and high efficiency, as was recently demonstrated [7,8]. However, these experiments utilized an electron beam that was much longer than the laser period, resulting in energy modulation rather than net acceleration. The question is therefore could we benefit from both worlds—namely, have net acceleration and at the same time high gradient in the DLA?

In order to achieve net acceleration, several research groups are considering generation of optically-spaced electron microbunches [9–14]. Novel schemes have been presented [9,10] as well as experimental demonstrations [11–14]. While the issue of generating optically-spaced electron microbunches is beyond the scope of this study, below we discuss a phenomenon common to all such schemes—beam loading.

Beam loading effect is slightly different in rf as compared to an optical regime. In most cases in rf machines, only one or very few microbunches exist in the acceleration module simultaneously [15–19], whereas in an optical regime hundreds or even thousands of microbunches may coexist in the accelerating module at any given moment. Therefore, in an optical regime the wake exerted on each microbunch may have a more significant effect.

As a result of this wake, there is a need for a tapered laser pulse in order to compensate for its effect. The tapering should take into account the laser's group velocity, which is much higher in DLA as compared to rf systems. The subject of compensating for beam loading by way of tailoring the driving rf pulse has been studied extensively over the years [20–22]. Among the common methods are either local [23] or global [24,25] correction schemes. However, to the best of our knowledge, systematic study of this subject in the context of dielectric laser accelerators (DLA) has not been pursued as of yet.

By leveraging beam loading effect, in part I of this study we proposed [26] a way to optimize a *single* bunch operation of DLA. We solved a self-consistent set of nonlinear constraints, taking into account the beam loading reduction on the material at the dielectric-vacuum interface; this case was referred to as the *reduced* case. For a given efficiency, the reduced case presented a higher loaded gradient than the un-reduced case (whereby the field reduction on the material is ignored). For example, maximum efficiency of 60.5% occurred for a loaded gradient of 6 GV/m in the reduced case, as compared with 2.5 GV/m in the unreduced case. In any case, the optimal charge to be accelerated was found to be a total of $\sim 10^6$ electrons in the bunch. Splitting the electron beam into a train of microbunches could be beneficial due to weakening the space

*Adiha@tx.technion.ac.il

charge effects and as a result, lead to some increase in the total amount of accelerated charge.

In the framework of this paper we repeat the self-consistent analysis presented in [26] for a *train* of microbunches, accounting for the beam loading reduction on the material (i.e., reduced case). The effect on the train is detrimental since different bunches experience different accelerating gradients. Therefore, in Sec. II we present an assessment of the beam loading effect on the bunch, and propose a way to compensate for it by *tapering* the laser pulse. Once tapered, the single bunch analysis still holds with a few adjustments as discussed in Sec. III, which also summarizes the results of the optimization procedure.

II. LASER PULSE TAPERING

Pursuant to our work on optimized operation of DLA with single bunch [26], we adopt an azimuthally symmetric dielectric-loaded waveguide [27], as shown in Fig. 1. However, in this configuration we split the single bunch into M microbunches ($q \to q = Mq_{\mathrm{mb}}$) with one wavelength spacing λ_{L} between adjacent microbunches. Neglecting space-charge, we tacitly assume that each microbunch is a point charge, and remains so all along the interaction region. Moreover, co-propagating with this train of relativistic microbunches, a single TM_{01} mode of a laser pulse traverses the accelerating structure with a phase velocity c and group velocity $\beta_{\mathrm{gr}}c$. The parameters for the numerical examples presented subsequently are summarized in Table I.

As in the single bunch case, there should be a full overlap between the laser pulse that propagates at $c\beta_{\mathrm{gr}}$ and the first microbunch in the train along the interaction length, $L_{\mathrm{geo}} = \Delta\gamma_{\mathrm{acc}} m_{\mathrm{e}} c^2/(eG_{\mathrm{loaded}})$, where $\Delta\gamma_{\mathrm{acc}}$ is the energy gain, m_{e} and e are the electron's mass and charge respectively. Thus, the delay time [29] between the two should be $\tau_{\mathrm{D}} \equiv L_{\mathrm{geo}}(\beta_{\mathrm{gr}}^{-1} - 1)/c$. Moreover, the pulse duration should be extended according to the number of microbunches, thus $\tau_{\mathrm{p}} = \tau_{\mathrm{D}} + \tau_{\mathrm{B}}$ where $\tau_{\mathrm{B}} \equiv (M-1)\lambda_{\mathrm{L}}/c$ is the bunch duration.

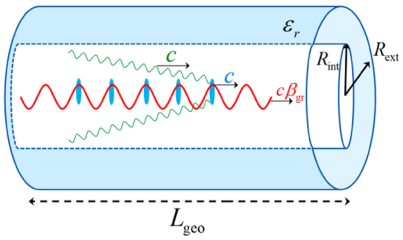

FIG. 1. Schematics of the basic principle and envisaged geometry. Five relativistic microbunches (blue) are accelerated by TM_{01} laser mode (red) which propagates at $c\beta_{\mathrm{gr}}$ group velocity, in a vacuum channel of a dielectric loaded cylinder. The wake (green), generated by the bunches, propagates at their velocity [28].

TABLE I. Parameters of the laser and the envisaged structure shown in Fig. 1.

Parameter	Symbol	Value
Laser		
Laser wavelength [μm]	λ_{L}	2
Group velocity	β_{gr}	0.5
Phase velocity	β_{ph}	1.0
Interaction impedance [Ω]	Z_{int}	325
Laser power [kW]	P_{L}	$6.1 \cdot \{G_0[\frac{\mathrm{GV}}{\mathrm{m}}]\}^2$
Structure		
Internal radius [λ_{L}]	R_{int}	0.47
External radius [λ_{L}]	R_{ext}	0.57
Dielectric constant	ε_{r}	3.9
Wake coefficient [$\frac{\mathrm{GV}}{\mathrm{m\cdot pC}}$]	κ	20.34
Energy gain required	$\Delta\gamma_{\mathrm{acc}}$	1.7
Maximum efficiency [%]	$\eta_{1,\mathrm{max}}$	60.5

For an assessment of the beam-loading effect we first need to establish the decelerating wakefield experienced by the νth microbunch given by

$$E_{\nu}^{\mathrm{wake}} \simeq Mq_{\mathrm{mb}}\kappa \times \sum_{s=1}^{\infty} W_s \left\langle \cos\left[2\pi\frac{\omega_s}{\omega_{\mathrm{L}}}(\nu - j)\right] 2h(\nu - j)\right\rangle_j \quad (1)$$

where W_s and ω_s are the weight and angular frequency of the s mode respectively ($\omega_{s=1} = \omega_{\mathrm{L}}$) [26], and $\langle \ldots \rangle_j = \frac{1}{M}\sum_{j=1}^{M} \ldots$; $h(u)$ is the Heaviside step function. Here we assume that the quality factor is large enough such that on the scale of the train duration, the decay associated with loss may be ignored, but is sufficiently low to facilitate bandwidth, which enables the propagation of the tapered pulse. Moreover, dispersion in the waveguide is ignored in the analysis.

Clearly, different microbunches experience different wakefield which in turn leads to substantial energy-spread—this is the beam-loading effect. In order to compensate for this detrimental effect, we need to adjust the laser pulse

$$G(\tau)[h(\tau + \tau_{\mathrm{D}}) - h(\tau - \tau_{\mathrm{B}})] \cos\left[\omega_{\mathrm{L}}\left(t - \frac{z}{c}\right)\right] \quad (2)$$

where $G(\tau \equiv t - z/c\beta_{\mathrm{gr}})$ is the laser's amplitude, and it is constant if the beam-loading is negligible. The major difficulty is now evident: the relativistic train of bunches moves at almost speed of light in vacuum, whereas the laser pulse's envelope travels at the group velocity, which can be quite smaller than c.

In order to eliminate the energy-spread deficiency, it is proposed to taper the laser's amplitude, thus instead of a constant accelerating gradient G_0, the tapered gradient is given by

$$G(\tau) = G_0 + \sum_{\nu=2}^{M} \Delta G_\nu h(\tau - T_{\mathrm{in},\nu-1}), \tag{3}$$

where ΔG_ν is the amplitude correction on the νth microbunch, which starts after the preceding microbunch entered the acceleration structure at $T_{\mathrm{in},\nu-1}$.

In principle, the amplitude corrections (ΔG_ν) are determined by minimizing the spread in the net kinetic energy gained by each microbunch, as compared with the first bunch ($\Delta G_1 = 0$), i.e., to minimize the functional

$$\sum_{\nu=1}^{M} [\Delta U_{\mathrm{kin},\nu} - \Delta U_{\mathrm{kin},1}]^2 \tag{4}$$

where $\Delta U_{\mathrm{kin},\nu} = q_{\mathrm{mb}} \int_{T_{\mathrm{in},\nu}}^{T_{\mathrm{in},\nu}+L_{\mathrm{geo}}/c} cdt[G(\tau) - E_\nu^{\mathrm{wake}}]$. The explicit analytic solution as well as an analytical example for $\beta_{\mathrm{gr}} = 0.5$ are given in Appendix A. Its main result is expressed in Eq. (5), but before we discuss it, we would like to emphasize that at the practical level, the required pulse shaping can be done in several ways: spatial light modulators, adaptive beam shaping, or fixed masks [30].

In what follows, we demonstrate the tapered amplitude required for a case wherein the tapered amplitude leads to a globally zero energy-spread for two values of β_{gr}. By global we mean that at the output-end all bunches emerge with the same energy-spread as they were at the input-end—in all cases considered the latter is zero. The first case to be considered, which is nonrealistic yet instructive, is when the laser propagates at the speed of light in vacuum ($\beta_{\mathrm{gr}} = 1$). In this case the tapered laser's amplitude should increase linearly in time. Explicitly, in terms of the formulation in Eq. (3), the tapered amplitude should satisfy $\Delta G_{\nu>1} = 2\kappa_1 q_{\mathrm{mb}}$.

For a typical group velocity value [31] of $\beta_{\mathrm{gr}} = 0.5$, the change in amplitude should satisfy

$$\Delta G_2 = 2\kappa_1 q_{\mathrm{mb}} \frac{L_{\mathrm{geo}}}{\lambda_{\mathrm{L}}} \tag{5}$$

and $\Delta G_{\nu>2} = 0$ otherwise. This leads to virtually zero *global* energy spread—see Appendix A. This laser pulse is a superposition of two components (as shown in Fig. 2): at the beginning a gradient G_0 is applied, and after the delay time τ_{D}, a ΔG_2 amplitude correction is added for the remainder of the pulse τ_{B}. In both cases, since the wake's nonfundamental modes are suppressed like $1/M^2$ [32] we considered only the first dominant mode of the wake ($\kappa \simeq \kappa_1$).

Figure 2 illustrates the propagating process of five microbunches in two time frames: top frame shows the case when the last bunch enters the structure and the lower frame reveals the conditions when the first bunch exits the interaction region. The time each microbunch spends in the "correction-zone" should compensate for the wake it experiences while traversing the structure. It is important to note that the gradient at the "correction-zone" is reduced by the train's wake, and therefore, it does not exceed the damage threshold fluence.

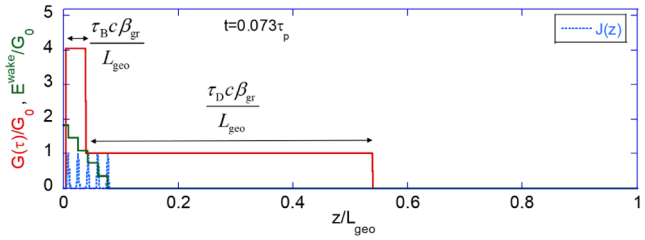

(a) Last microbunch enters the structure.

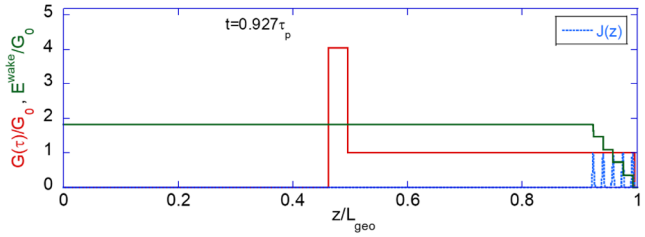

(b) First microbunch exits the structure.

FIG. 2. Laser pulse's envelope (red), normalized to $G_0 = 8$ GV/m, propagates at $\beta_{\mathrm{gr}} = 0.5$, while the wake (green), generated by five relativistic microbunches (blue), propagates at their velocity. The above three quantities are presented for two different time frames: (a) last microbunch enters the structure, (b) first microbunch exits it. First, a gradient G_0 is applied for a delay time τ_{D}, and then a $3G_0$ amplitude correction is added for the remainder of the pulse. The time each microbunch spends in such "correction-zone" compensates for the wake it experiences while traversing the structure.

Two facts are evident: first, it is impossible to locally taper the laser for $\beta_{\mathrm{gr}} < 1$. Therefore, for the latter case the laser is tapered *globally* in a way that the effective loaded gradient as experienced by the microbunches during the time they traverse the accelerating module is the same. Second, when the microbunches enter the structure, the laser pulse might be half a way in the structure [as shown in Fig. 2(a)], while no wake has been generated in this region to reduce the intense optical field the dielectric is exposed to. During this time period, the field at the dielectric interface may be higher than the damage threshold fluence. Therefore, the latter would set an upper limit on the unloaded gradient values (G_0).

III. SELF-CONSISTENT ANALYSIS

In this section we self-consistently determine the optimal charge, efficiency, and gradient for laser driven accelerators in a case of train of microbunches. After establishing the amplitude tapering of the laser pulse to compensate for the beam-loading effect on the train of M bunches, the loaded gradient that acts on each microbunch is $G_{\mathrm{loaded}} = G_0 - \kappa q_{\mathrm{mb}}$—same as in single bunch. Therefore, we are now in a position to repeat the approach developed for a single bunch [26] to a train of multiple bunches. In what

follows we present the results of the reduced case only, whereby the beam loading reduction on the vacuum-dielectric interface was taking into account.

With these adaptations, single bunch analysis still holds; given $\Delta\gamma_{\mathrm{acc}}$, the vacuum channel's radius (R_{int}), the group velocity (β_{gr}), the laser wavelength (λ), and the geometrical length of the structure (L_{geo}), we can establish the gradient and optimal charge to be accelerated for various number of microbunches in the train (M), in a *self-consistent* way.

The efficiency of this paradigm $(\eta_M \equiv \sum_\nu \Delta U_{\mathrm{kin},\nu}/U_{\mathrm{EM}})$, should include the electromagnetic energy (U_{EM}) in the tapered laser pulse, and as shown in Appendix B it is given by

$$\frac{\eta_M}{\eta_{1,\max}} = \frac{\left[4\frac{\kappa q_{\mathrm{mb}}}{G_0}\left(1-\frac{\kappa q_{\mathrm{mb}}}{G_0}\right)\right]M}{1+\frac{\lambda_{\mathrm{L}}}{L_{\mathrm{geo}}}\frac{\beta_{\mathrm{gr}}}{1-\beta_{\mathrm{gr}}}\sum_{\nu=2}^{M}\left(1+\sum_{\mu=2}^{\nu}\frac{\Delta G_\mu}{G_0}\right)^2}. \quad (6)$$

where $\eta_{1,\max} \equiv \kappa_1/\kappa$ is the single bunch maximum efficiency [29,32,33] determined by the structure—see Table I.

Figure 3a shows the train of bunches efficiency normalized to the single bunch maximum efficiency $(\eta_{1,\max} = 60.5\%)$ as a function of the loaded gradient (bottom X-axis) or the structure's geometric length (top X-axis). Each curve represents a different number of bunches in the train: single bunch $M = 1$ (dotted green), $M = 2$ (red), $M = 10$ (dashed

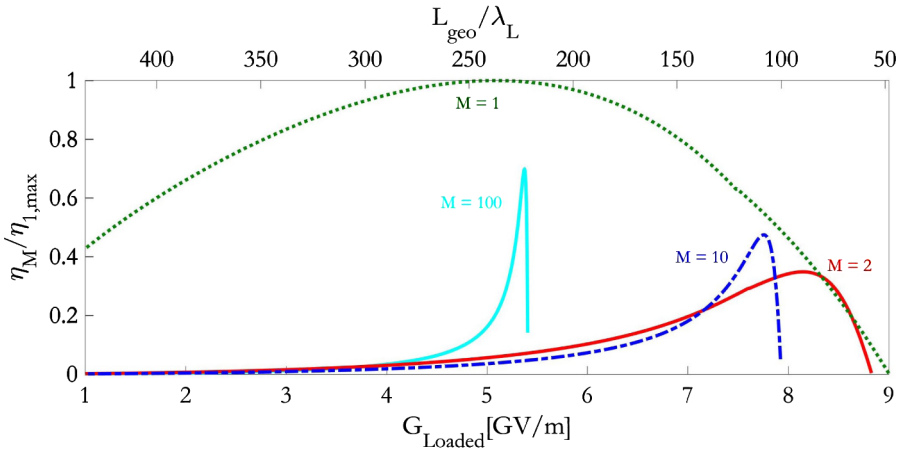

(a) Geometric length dependence. Notably, the maximum efficiency for $M = 2$ drops to $\sim 40\%$ as compared with the maximum efficiency of single bunch, due to the electromagnetic energy in the tapered pulse. Moreover, the maximum loaded gradient decreases for long trains $(M = 100)$.

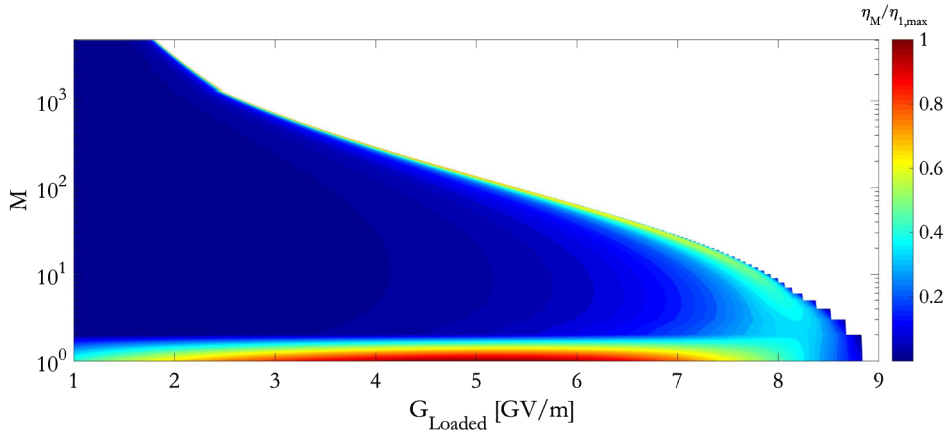

(b) Multi-bunch continuum dependence. Notably, loaded gradient which occurs for maximum efficiency is smaller than the maximum gradient the structure can sustain for low number of microbunches. However, for a long train $(M \to 10^3)$ this difference diminishes. Maximum efficiency for long train of bunches is 20% lower than the maximum single bunch efficiency.

FIG. 3. (a) Efficiency normalized to the single bunch maximum efficiency $(\eta_{1,\max} = 60.5\%)$ as a function of the loaded gradient (bottom X-axis) or the structure's geometric length (top X-axis). Each curve represents a different number of bunches in the train: single bunch $M = 1$ (dotted green), $M = 2$ (red), $M = 10$ (dashed blue), and $M = 100$ (cyan). (b) Contours of efficiency η_{M} as a function of number of bunches in the train and the corresponding loaded gradient. Other simulations parameters are summarized in Table I.

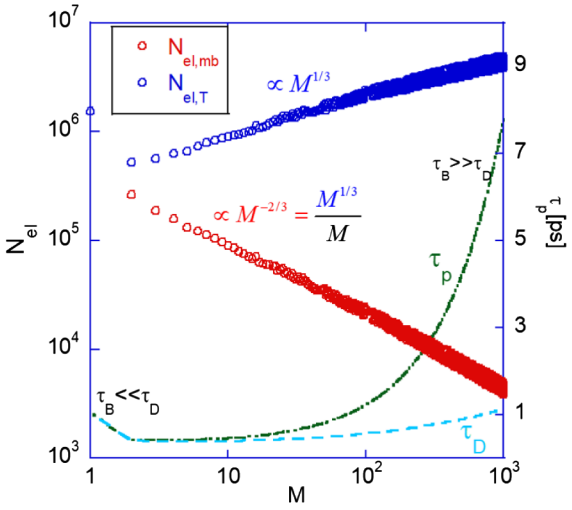

FIG. 4. Left vertical axis: Total optimal charge in the train (blue) increases moderately as a function of number of microbunches in the train (M), while the charge in a microbunch (red) decreases by two orders of magnitude. Right vertical axis: Pulse length (green) and delay time (dashed turquoise) for which maximum efficiency and optimal charge occur.

blue), and $M = 100$ (cyan). Notably, the maximum efficiency for train $(M > 1)$ of bunches (η_{M}) is reduced as compared with the maximum efficiency of single bunch, due to the electromagnetic energy in the tapered pulse. For example, η_{M} drops to $0.4\eta_{1,\mathrm{max}}$ for two bunches, but somewhat recovers to 70% for longer trains $(M = 100)$, which also occurs for longer structures. It is also evident that the maximum loaded gradient decreases for long trains. In addition, maximum efficiency for each M occurs for a different structure length.

In order to understand the effect of multiple bunches, Fig. 3(b) presents contours of the normalized train efficiency as a function of the number of bunches in the train M, and the corresponding loaded gradient. This figure shows that the maximum loaded gradient may reach 9 GV/m for low values of M, and changes by a factor of ~5 with the number of microbunches in the train (M).

Furthermore, one should distinguish between maximum gradient and gradient for maximal efficiency. For low number of microbunches, gradient which occurs for maximum efficiency is smaller than the maximum gradient the structure can sustain. However, for a long train $(M \to 10^3)$ this difference diminishes. A similar trend was observed for the *efficiency*; its values for maximal gradient $(< 0.02\eta_{1,\mathrm{max}})$ are significantly small as compared with the maximum value attainable. Second, maximum efficiency of single bunch $(\eta_{1,\mathrm{max}})$ is at least 20% higher than the train case. Lastly, since the maximum efficiency and maximum loaded gradient do not occur for the same conditions, compromised values for *both* are $0.7\eta_{1,\mathrm{max}}$ and $G_{\mathrm{Loaded}} = 6$ GV/m, which occur for $M \simeq 100$ microbunches in the train.

Another perspective of the energy conversion efficiency is the amount of *charge* accelerated. Optimal charge for microbunch in the train, calculated for maximum efficiency, varies moderately as a function of the number of microbunches (M). Figure 4 shows the total number of electrons (N_{el}) in the train (blue circles) monotonically increases as $M^{1/3}$, and ranges between $0.5\times10^6-5\times10^6$. Nevertheless, the number of electrons in a microbunch (red circles) drops by two orders of magnitude. This behavior could be explained by the fact that the analysis is highly nonlinear: as was shown in Fig. 3(a), maximum efficiency for long trains occurs for longer structures. For the latter, the microbunch charge which occurs for the maximum efficiency decreases as was shown in Part I of this study [26]. Therefore, the microbunch charge decreases with M. As a result, the loading would be more significant for short train of bunches, and thus the loaded gradient on the bunch would be smaller, as was previously shown in Fig. 3(b).

Finally, the pulse length for which the maximum efficiency occurs (green curve in Fig. 4) changes with the number of microbunches in the train. As a consequence, the delay time (dashed turquoise) also varies with M, since its depends on the geometrical length, and the latter depends on M in the multi-bunch case.

IV. CONCLUSION

In conclusion, our *self-consistent* analysis for a train of microbunches reveals that there is a total charge of $0.5 \times 10^6 - 5 \times 10^6$ electrons in the train, regardless of the number of microbunches. Analytical solution is achievable for $\beta_{\mathrm{gr}} = 0.5$, whereby the maximum efficiency attainable with a train of microbunches is at least 20% lower than the single bunch case. The properties of the latter's three different regimes of operation were presented in our previous work [34].

It has been shown that beam loading effect on the train of M microbunches can be globally compensated by a tapered laser pulse. Further, the beam loading reduction on the material was also considered. This case, previously referred to as the reduced case [26], exhibited maximum loaded gradients which vary between ~2 for long trains $(M > 10^3)$, and ~10 GV/m for short trains $(M < 10)$. A trade-off between maximum efficiency and maximum gradient, as a function of number of microbunches in the train, has been suggested.

Beyond pure high energy physics applications, a train of accelerated microbunches may pave the way to a novel regime of light sources, whereby the microbunches' spacing is in the infrared laser wavelength, and the microbunch length might facilitate bursts of deep ultraviolet radiation.

ACKNOWLEDGMENTS

This study was supported by Israel Science Foundation and Rothschild Caesarea Foundation.

APPENDIX A: MINIMIZING ENERGY-SPREAD—ANALYTIC SOLUTION

In this Appendix we determine the amplitudes of the tapered laser (ΔG_ν) by minimizing the spread in the net kinetic energy gained by each microbunch compared to the first bunch, i.e., minimizing the functional

$$\delta(\overrightarrow{\Delta G}) = \sum_{\nu=1}^{M} [\Delta U_{\mathrm{kin},\nu} - \Delta U_{\mathrm{kin},1}]^2 \tag{A1}$$

where $\Delta U_{\mathrm{kin},\nu} = q_{\mathrm{mb}} \int_{T_{\mathrm{in},\nu}}^{T_{\mathrm{in},\nu}+L_{\mathrm{geo}}/c} cdt[G(\tau) - E_\nu^{\mathrm{wake}}]$, E_ν^{wake} is the decelerating wakefield experienced by the νth microbunch, and

$$G(\tau) = G_0 + \sum_{\nu=2}^{M} \Delta G_\nu h(\tau - T_{\mathrm{in},\nu-1}). \tag{A2}$$

ΔG_ν is the amplitude correction on the νth microbunch, $T_{\mathrm{in},\nu}$ is the time for which the νth microbunch enters the acceleration structure, and $h(\tau)$ is the Heaviside step function [$h(\tau > 0) = 1$, $h(\tau = 0) = 0.5$, and zero elsewhere].

Defining

$$H_{\nu,\mu} \equiv \int_{T_{\mathrm{in},\nu}}^{T_{\mathrm{in},\nu}+\frac{L_{\mathrm{geo}}}{c}} dth\left(t - \frac{ct - \lambda_{\mathrm{L}}(\nu-1)}{c\beta_{\mathrm{gr}}} - T_{\mathrm{in},\mu-1}\right)$$
$$\mathrm{K}_\nu \equiv \int_{T_{\mathrm{in},\nu}}^{T_{\mathrm{in},\nu}+\frac{L_{\mathrm{geo}}}{c}} dtE_\nu^{\mathrm{wake}} + \int_{T_{\mathrm{in},1}}^{T_{\mathrm{in},1}+\frac{L_{\mathrm{geo}}}{c}} dtE_1^{\mathrm{wake}} \tag{A3}$$

the error, $\delta(\overrightarrow{\Delta G})$, is

$$c^2 q_{\mathrm{mb}}^2 \sum_{\nu=1}^{M} \left[\sum_{\mu=1}^{M}(H_{\nu,\mu} - H_{1,\mu})\Delta G_\mu - \mathrm{K}_\nu\right]^2. \tag{A4}$$

Minimizing the error for each correction, i.e., $\mathrm{dError}(\overrightarrow{\Delta G})/d\Delta G_\sigma = 0$, results in $\overrightarrow{\Delta G} = \mathrm{Mat}^{-1}\vec{S}$ where Mat^{-1} is the inverse of the matrix $\mathrm{Mat}_{\sigma,\mu} \equiv \sum_{\nu=1}^{M}(H_{\nu,\mu} - H_{1,\mu})(H_{\nu,\sigma} - H_{1,\sigma})$ and $S_\sigma \equiv \sum_{\nu=1}^{M} \mathrm{K}_\nu(H_{\nu,\sigma} - H_{1,\sigma})$. This procedure leads to zero energy spread globally, namely that at the output-end all bunches emerge with the same energy-spread as they were at the input-end.

As an analytic example, the amplitude's corrections for $\beta_{\mathrm{gr}} = 0.5$ are given by

$$\Delta G_\nu = \frac{L_{\mathrm{geo}}}{\lambda_{\mathrm{L}}} 2\kappa q \sum_{s=1}^{\infty} W_s[X_s(1) - X_s(2)] \tag{A5}$$

where

$$X_s(j) = \cos\left[2\pi(\nu - j)\frac{\omega_s}{\omega_{\mathrm{L}}}\right]\Theta(\nu - j), \tag{A6}$$

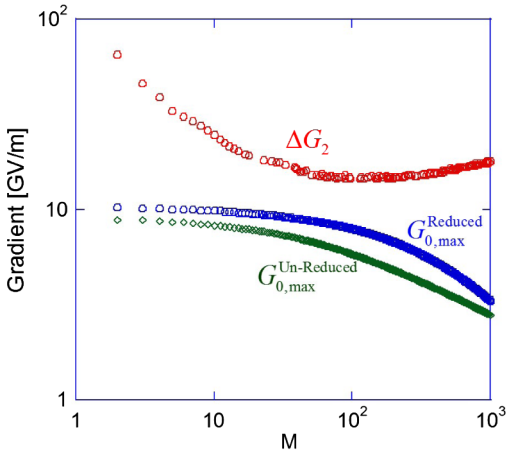

FIG. 5. The amplitude correction ΔG_2 (red) dependence on the number of bunches in the train for the optimal charge in Fig. 4. Moreover, the maximum unloaded gradient for the reduced case (blue) is higher than the one for the unreduced case (green).

$\Theta(x > 0) = 1$, and zero elsewhere, and W_s are the wake's weight functions. Consider only the first dominant mode ($s = 1$), the latter is reduced to $\Delta G_2 = 2\kappa_1 q_{\mathrm{mb}} L_{\mathrm{geo}}/\lambda_{\mathrm{L}}$ and $\Delta G_{\nu>2} = 0$.

Figure 5 shows the latter amplitude correction ΔG_2 (red) dependence on the number of bunches in the train for the optimal charge shown in FIG. 4 (which occurs for maximum efficiency). Note that, due to nonlinear dependence of q_{mb}, L_{geo}, and M, although q_{mb} decreases like $M^{-2/3}$, the amplitude correction $\Delta G_2 \propto q_{\mathrm{mb}}(L_{\mathrm{geo}})L_{\mathrm{geo}}$ does not decrease monotonically, but rather has a minimum point at $M \simeq 100$. This would allow to work with a laser with a minimal change in amplitude. Effectively, the structure's material would not experience this amplitude correction since it will be canceled by the bunch's wake. Moreover, as expected, the maximum unloaded gradient for the reduced case (blue) is higher than the one for the un-reduced case (green).

APPENDIX B: EFFICIENCY DERIVATION FOR A TRAIN OF MICROBUNCHES

In this Appendix we derive the expression in Eq. (6) for the efficiency of train of microbunches. In general, the efficiency of train of microbunches is a measure to the increase in the net kinetic energy of *all* the microbunches, relative to the electromagnetic energy U_{EM} in the tapered laser pulse

$$\eta_M \equiv \frac{\sum_\nu \Delta U_{\mathrm{kin},\nu}}{U_{\mathrm{EM}}}. \tag{B1}$$

The electromagnetic energy in the tapered pulse is

$$U_{\mathrm{EM}} = \int_{-\tau_D}^{\tau_B} d\tau P_{\mathrm{L}}(\tau) = \int_{-\tau_D}^{\tau_B} d\tau \frac{|\lambda_{\mathrm{L}} G(\tau)|^2}{Z_{\mathrm{int}}} \tag{B2}$$

where P_L is the laser power, and

$$G(\tau) = G_0 + \sum_{\nu=2}^{M} \Delta G_\nu h(\tau - T_{\mathrm{in},\nu-1}) \tag{B3}$$

is the tapered laser amplitude. Substituting the latter into Eq. (B2) and integrating, we get

$$\Delta U_{\mathrm{EM}} = \frac{|\lambda_L|^2 G_0^2}{Z_{\mathrm{int}}} \left[\tau_D + \sum_{\nu=2}^{M} \left(1 + \sum_{\mu=2}^{\nu} \frac{\Delta G_\mu}{G_0} \right)^2 \frac{\lambda_L}{c} \right]. \tag{B4}$$

The net kinetic energy for the νth microbunch is given by

$$\Delta U_{\mathrm{kin},\nu} = q_{\mathrm{mb}} c \int_{(\nu-1)\frac{\lambda_L}{c}}^{\frac{(\nu-1)\lambda_L + L_{\mathrm{geo}}}{c}} dt [G_0 - \kappa q + E_\nu^{\mathrm{taper}} - E_\nu^{\mathrm{wake}}]. \tag{B5}$$

Since the tapered amplitude E_ν^{taper} for each microbunch νth was determined to compensate for the decelerating wakefield it experiences (see Sec. II), the net kinetic energy for all microbunches is

$$\sum_\nu \Delta U_{\mathrm{kin},\nu} = M \langle \Delta U_{\mathrm{kin},\nu} \rangle_\nu \simeq M q_{\mathrm{mb}} (G_0 - \kappa q) L_{\mathrm{geo}}. \tag{B6}$$

Therefore the efficiency of train of microbunches is

$$\begin{aligned} \eta_M &= \frac{M q_{\mathrm{mb}} [G_0 - \kappa q_{\mathrm{mb}}] L_{\mathrm{geo}}}{\frac{|\lambda_L|^2 G_0^2}{Z_{\mathrm{int}}} \left[\tau_D + \sum_{\nu=2}^{M} \left(1 + \sum_{\mu=2}^{\nu} \frac{\Delta G_\mu}{G_0} \right)^2 \frac{\lambda_L}{c} \right]} \\ &= \frac{Z_{\mathrm{int}} L_{\mathrm{geo}}}{|\lambda_L|^2 \kappa} \frac{\frac{\kappa q_{\mathrm{mb}}}{G_0} \left(1 - \frac{\kappa q_{\mathrm{mb}}}{G_0} \right) M}{\tau_D + \sum_{\nu=2}^{M} \left(1 + \sum_{\mu=2}^{\nu} \frac{\Delta G_\mu}{G_0} \right)^2 \frac{\lambda_L}{c}} \end{aligned} \tag{B7}$$

Substituting the definition for the delay time (τ_D), Eq. (B7) is reduced to

$$\frac{Z_{\mathrm{int}} L_{\mathrm{geo}} c}{|\lambda_L|^2 \kappa} \frac{\frac{\kappa q_{\mathrm{mb}}}{G_0} \left(1 - \frac{\kappa q_{\mathrm{mb}}}{G_0} \right) M}{L_{\mathrm{geo}} (\beta_{\mathrm{gr}}^{-1} - 1) + \lambda_L \sum_{\nu=2}^{M} \left(1 + \sum_{\mu=2}^{\nu} \frac{\Delta G_\mu}{G_0} \right)^2} \tag{B8}$$

Keeping in mind that the projection of the wake on the fundamental mode is given by $\kappa_1 = Z_{\mathrm{int}} c \beta_{\mathrm{gr}} / 4\lambda_L^2 (1 - \beta_{\mathrm{gr}})$ [35], Eq. (B8) is reduced to

$$\begin{aligned} \eta_M &= 4 \frac{\kappa_1}{\kappa} \frac{\frac{\kappa q_{\mathrm{mb}}}{G_0} \left(1 - \frac{\kappa q_{\mathrm{mb}}}{G_0} \right) M}{1 + \frac{\lambda_L}{L_{\mathrm{geo}}} \frac{\beta_{\mathrm{gr}}}{1 - \beta_{\mathrm{gr}}} \sum_{\nu=2}^{M} \left(1 + \sum_{\mu=2}^{\nu} \frac{\Delta G_\mu}{G_0} \right)^2} \\ &= \eta_{1,\max} \frac{4 \frac{\kappa q_{\mathrm{mb}}}{G_0} \left(1 - \frac{\kappa q_{\mathrm{mb}}}{G_0} \right) M}{1 + \frac{\lambda_L}{L_{\mathrm{geo}}} \frac{\beta_{\mathrm{gr}}}{1 - \beta_{\mathrm{gr}}} \sum_{\nu=2}^{M} \left(1 + \sum_{\mu=2}^{\nu} \frac{\Delta G_\mu}{G_0} \right)^2}. \end{aligned} \tag{B9}$$

This is the same as Eq. (6), and is reduced to the single bunch efficiency for $M = 1$.

[1] W. Kimura, A. van Steenbergen, M. Babzien, I. Ben-Zvi, L. Campbell, D. Cline, C. Dilley, J. Gallardo, S. Gottschalk, P. He, K. Kusche, Y. Liu, R. Pantell, I. Pogorelsky, D. Quimby, J. Skaritka, L. Steinhauer, and V. Yakimenko, First Staging of Two Laser Accelerators, Phys. Rev. Lett. **86**, 4041 (2001).

[2] C. M. Sears, E. Colby, R. J. England, R. Ischebeck, C. McGuinness, J. Nelson, R. Noble, R. H. Siemann, J. Spencer, D. Walz, T. Plettner, and R. L. Byer, Phase stable net acceleration of electrons from a two-stage optical accelerator, Phys. Rev. ST Accel. Beams **11**, 101301 (2008).

[3] M. Dunning, E. Hemsing, C. Hast, T. O. Raubenheimer, S. Weathersby, D. Xiang, and F. Fu, Demonstration of Cascaded Optical Inverse Free-Electron Laser Accelerator, Phys. Rev. Lett. **110**, 244801 (2013).

[4] R. J. England, R. J. Noble, B. Fahimian, B. Loo, E. Abel, A. Hanuka, and L. Schachter, Conceptual layout for a wafer-scale dielectric laser accelerator , AIP Conf. Proc. **1777**, 060002 (2016).

[5] V. Karagodsky and L. Schächter, High efficiency x-ray source based on inverse Compton scattering in an optical Bragg structure, Plasma Phys. Controlled Fusion **53**, 014007 (2011).

[6] T. Plettner and R. L. Byer, Proposed dielectric-based microstructure laser-driven undulator, Phys. Rev. ST Accel. Beams **11**, 030704 (2008).

[7] E. A. Peralta, K. Soong, R. J. England, E. R. Colby, Z.Wu, B. Montazeri, C. McGuinness, J. McNeur, K. J. Leedle, D.Walz, E. B. Sozer, B. Cowan, B. Schwartz, G. Travish, and R. L. Byer, Demonstration of electron acceleration in a laser-driven dielectric microstructure, Nature (London) **503**, 91 (2013).

[8] K. Wootton, Z. Wu, B. Cowan, A. Hanuka, I. Makasyuk, E. Peralta, K. Soong, R. Byer, and R. England, Demonstration of acceleration of relativistic electrons at a dielectric microstructure using femtosecond laser pulses, Opt. Lett. **41**, 2696 (2016).

[9] F. Süßmann, M. F. Kling, and P. Hommelhoff, in *Attosecond Nanophysics: From Basic Science to Applications* (Wiley-VCH Ve, Germany, 2014), ch. 6.

[10] L. Schächter, W. Kimura, and I. Ben-Zvi, Ultrashort microbunch electron source, AIP Conf. Proc. **1777**, 080013 (2016).

[11] C. Sears, E. Colby, R. Ischebeck, C. McGuinness, J. Nelson, R. Noble, R. Siemann, J. Spencer, D. Walz, T. Plettner, and R. Byer, Production and characterization of attosecond electron bunch trains, Phys. Rev. ST Accel. Beams **11**, 061301 (2008).

[12] X. E. Lu, C. E. Tang, R. E. Li, H. To, G. Andonian, and P. Musumeci, Generation and measurement of velocity bunched ultrashort bunch of pC charge, Phys. Rev. ST Accel. Beams **18**, 032802 (2015).

[13] D. Xiang, E. Hemsing, M. Dunning, C. Hast, and T. Raubenheimer, Femtosecond Visualization of Laser-Induced Optical Relativistic Electron Microbunches, Phys. Rev. Lett. **113**, 184802 (2014).

[14] P. Muggli, V. Yakimenko, M. Babzien, E. Kallos, and K. P. Kusche, Generation of Trains of Electron Microbunches with Adjustable Subpicosecond Spacing, Phys. Rev. Lett. **101**, 054801 (2008).

[15] ILC, Stanford Technical Report No. SLAC-R-857, 2007.

[16] J. Hao, S. Quan, X. Lu, F. Zhu, L. Lin, B. Zhang, K. Zhao, K. Liu, and J. Chen, SRF activities at Peking University, *Proceedings of SRF2011, Chicago, USA* (2011), p. 969–972.

[17] S. Belomestnykh, Y. Hao, V. Litvinenko, V. Ptitsyn, and W. Xu, On the frequency choice for thr eRHIC SRF LINAC, *Proceedings of IPAC2014, Dresden, Germany* (2014), p. 1547–1549.

[18] S. Liu, M. Fukuda, S. Araki, N. Terunuma, J. Urakawa, K. Hirano, and N. Sasao, Beam loading compensation for acceleration of multi-bunch electron beam train, Nucl. Instrum. Methods Phys. Res., Sect. A **584**, 1 (2008).

[19] P. Muggli, B. Allen, V. E. Yakimenko, J. Park, M. Babzien, K. P. Kusche, and W. D. Kimura, Simple method for generating adjustable trains of picosecond electron bunches, Phys. Rev. ST Accel. Beams **13**, 052803 (2010).

[20] R. M. Jones, V. A. Dolgashev, and J. W. Wang, Dispersion and energy compensation in high-gradient linacs for lepton colliders, Phys. Rev. ST Accel. Beams **12**, 051001 (2009).

[21] N. Towne and J. Rose, Beam loading compensation of traveling wave linacs through the time dependence of the rf drive, Phys. Rev. ST Accel. Beams **14**, 090402 (2011).

[22] A. Lunin, V. Yakovlev, and A. Grudiev, Analytical solutions for transient and steady state beam loading in arbitrary traveling wave accelerating structures, Phys. Rev. ST Accel. Beams **14**, 052001 (2011).

[23] Z. Li, R. Miller, D. Farkas, T. Raubenheimer, H. Tang, and D. Yeremian, Stanford Technical Report No. SLAC-PUB-7429, 1997.

[24] S. Kashiwagi, H. Hayano, F. Hinode, K. Kubo, H. Matsumoto, S. Nakamura, T. Naito, K. Oide, K. Takata, S. Takeda, N. Terunuma, J. Urakawa, T. Okugi, and M. Kagaya, Preliminary test of +- F energy compensation system, in *Proc. of the 18th Int. Linac Conf.* (Geneva, 1996) p. 848.

[25] M. Satoh, T. Matsumoto, T. Shidara, S. Fukuda, H. Kobayashi, Y. Kamiya, N. Nakamura, T. Koseki, and S. Miura, Initial-beam-loading compensation system for high-intensity electron linacs, Nucl. Instrum. Methods Phys. Res., Sect. A **538**, 116 (2005).

[26] A. Hanuka and L. Schachter, , Phys. Rev. Accel. Beams **21**, 054001 (2018).

[27] M. Rosing and W. Gai, Longitudinal- and transverse-wake-field effects in dielectric structures, Phys. Rev. D **42**, 1829 (1990).

[28] L. Schachter, *Beam-Wave Interaction in Periodic and Quasi-Periodic Structures* (Springer, Berlin, Heidelberg, 2011).

[29] L. Schächter, Energy recovery in an optical linear collider, Phys. Rev. E **70**, 016504 (2004).

[30] C. Chang, J. Liang, D. Hei, M. F. Becker, K. Tang, Y. Feng, V. Yakimenko, C. Pellegrini, and J. Wu, High-brightness X-ray free-electron laser with an optical undulator by pulse shaping , Opt. Express **21**, 32013 (2013).

[31] T. Plettner, P. P. Lu, and R. L. Byer, Proposed few-optical cycle laser-driven particle accelerator structure, Phys. Rev. ST Accel. Beams **9**, 111301 (2006).

[32] A. Hanuka and L. Schächter, Bragg accelerator optimization, High Power Laser Sci. Eng. **2**, e24 (2014).

[33] R. H. Siemann, Energy efficiency of laser driven, structure based accelerators, Phys. Rev. ST Accel. Beams **7**, 061303 (2004).

[34] A. Hanuka and L. Schächter, Operation regimes of a dielectric laser accelerator, Nucl. Instrum. Methods Phys. Res., Sect. A **888**, 147 (2018).

[35] K. Bane and G. Stupakov, Impedance of a rectangular beam tube with small corrugations, Phys. Rev. ST Accel. Beams **6**, 024401 (2003).